PHYSICAL REVIEW A **77**, 060701(R) (2008)

Fine-structure-changing collisions in atomic titanium

Mei-Ju Lu, Kyle S. Hardman, and Jonathan D. Weinstein*
Department of Physics, University of Nevada, Reno, Nevada 89557, USA

Bernard Zygelman
Department of Physics and Astronomy, University of Nevada, Las Vegas, Nevada 89154, USA

(Received 6 December 2007; published 10 June 2008)

We have measured cold titanium-helium collisions that cause transitions between the fine-structure levels of the $[3d^24s^2]\ ^3F_J$ electronic ground state of atomic titanium, over a temperature range from 5 to 20 K. The Ti-He inelastic collision cross section is significantly smaller than cross sections measured for collisions of non-transition-metal atoms with noble gas atoms. Our theoretical calculations of the inelastic cross sections reproduce the magnitude and temperature dependence of the measurements, and attribute the suppression of inelastic collisions to titanium's "submerged" *d*-shell valence electrons.

DOI: 10.1103/PhysRevA.77.060701 PACS number(s): 34.50.−s, 32.80.Xx, 34.20.−b, 95.30.Dr

Fine-structure-changing collisions have long been of experimental and theoretical interest. The collisional excitation of fine-structure levels contributes to the cooling of diffuse interstellar gas and planetary atmospheres [1,2]. Typical rate coefficients for fine-structure relaxation for atoms such as oxygen, carbon, silicon, and aluminum in collisions with noble gases or atomic hydrogen range from 10^{-12} to 10^{-10} cm^3 s^{-1} [3–5].

There is renewed interest in the collisional interaction of atoms with fine structure due to the development of new methods to cool and trap ground-state or metastable-state atoms with nonzero orbital angular momentum [6–8]. Atoms with nonzero orbital angular momentum have an anisotropic interaction potential, and consequently are expected to exhibit large inelastic collision cross sections [9,10]. An experiment with laser-cooled metastable $[4s4p]\ ^3P_2$ calcium atoms confirmed these expectations by measuring very large inelastic Ca*-Ca* collision rates at ultracold temperatures [7]. But because the experiment studied trap loss from a magnetic trap, it was unable to distinguish inelastic Zeeman relaxation collisions (*m*-changing collisions) from inelastic fine-structure collisions (*J*-changing collisions). The relative strength of these two collisional processes remains an open question [7]. Understanding the nature of these collisional interactions is crucial for realizing new regimes of quantum degenerate gases with anisotropic interactions.

Recent experiments measuring Ti-He collisions [11,12] observed a dramatic suppression of *m*-changing collisions due to titanium's submerged shell structure. The *ab initio* Ti-He potential calculations of Kłos *et al.* suggest that titanium may exhibit a similar suppression of fine-structure-changing collisions [13]. In this work, we experimentally demonstrate this suppression, measure the inelastic collision rate coefficient, measure the ratio of *m*- and *J*-changing collisions, and confirm the origin of the suppression effect through theoretical calculations. The enhanced collisional stability indicates excited fine-structure states in submerged-shell atoms may be of use in future ultracold atom experiments.

*weinstein@physics.unr.edu

In our experiments, we laser ablate a titanium target to produce titanium atoms, and use a cryogenic helium buffer gas to rapidly cool their translational temperature [14–17]. A schematic of the experiment is shown in Fig. 1.

The ground electronic state of titanium is $[3d^24s^2]\ a\ ^3F_J$, with two $3d$ valence electrons below the filled $4s$ subshell. This state has fine-structure levels $J=2$, 3, and 4 at energies 0, 170, and 387 cm^{-1}, respectively [18]. We measure the population of the fine-structure levels of the electronic ground-state titanium atoms by absorption spectroscopy on the $[3d^24s^2]\ a\ ^3F_J \rightarrow [3d^24s4p]\ y\ ^3F_J$ transitions. A simplified diagram of the relevant energy levels is shown in Fig. 2 with a spectrum of the $J=2$ ground-state level.

The translational temperature of the titanium atoms is measured by fitting measured spectra to the expected Voigt line shape. The atoms were observed to translationally thermalize on a time scale of roughly a few 100 microseconds. This time scale varies with ablation conditions and helium density. We wait many thermalization times before making collision measurements to ensure the titanium atoms are

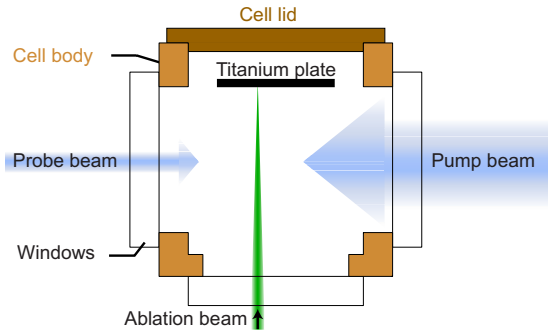

FIG. 1. (Color online) Apparatus schematic. The cell body is a six-way copper cross. Five of the faces are sealed with 3 inch diameter windows, and the sixth is sealed with a brass lid which carries a titanium ablation target. The cell is connected to a pulse tube cooler via a copper heatlink (not shown). The cell sits in vacuum and is filled with helium gas through a stainless steel tube (not shown). Probe and pump beams are generated by a grating-stabilized diode laser. Typical probe powers are a few microwatts, typical pump powers are a few milliwatts.

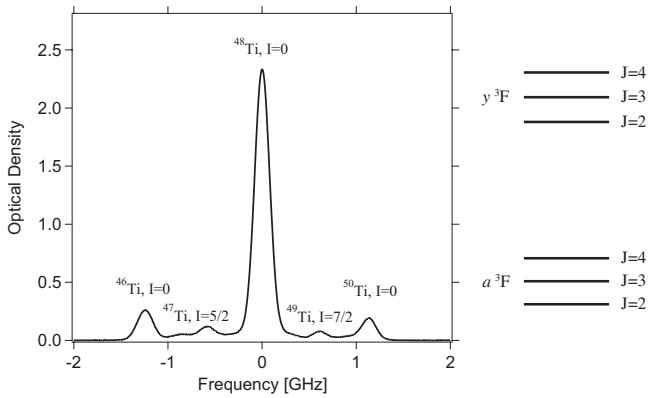

FIG. 2. Simplified Ti level diagram, alongside an absorption spectrum of ground-state titanium atoms taken on $[3d^24s^2]\ a\ ^3F_2 \rightarrow [3d^24s4p]\ y\ ^3F_2$ transition. The frequency offset in the graph is 25 107 cm^{-1}. The spectrum was taken 0.2 s after the laser ablation pulse at a cell temperature of 5.2 K. The frequency calibration is obtained from a Fabry-Perot cavity. The uncertainty in the frequency scale is ±5%, predominantly from nonlinearity in the laser scan. The titanium target consists of natural abundance titanium isotopes; the hyperfine lines are labeled according to isotope. All collision data in this paper is for the ^{48}Ti isotope.

translationally thermalized. The cell temperature is measured independently by a calibrated silicon diode [19], and the two temperature measurements are consistent within our experimental error.

Our primary method of measuring inelastic collisions is to perturb the titanium atom distribution by optical pumping and observe their return to thermal equilibrium through inelastic collisions [17]. After thermalization of the titanium's translational temperature, we turn on a high intensity optical pumping beam tuned to the $a\ ^3F_2 \rightarrow y\ ^3F_2$ transition at 25 107 cm^{-1} to transfer population from the $J=2$ ground state to $J=3$ [18]. By measuring the return to equilibrium, as shown in Fig. 3, we determine the $J=3 \rightarrow J=2$ inelastic collision rate.

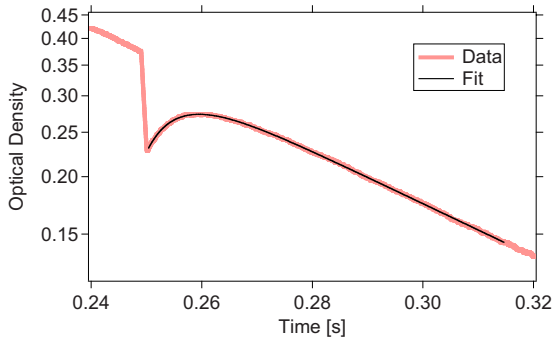

FIG. 3. (Color online) Absorption spectroscopy of ^{48}Ti atoms in the $a\ ^3F_2$ state, showing a return to equilibrium following an optical pumping pulse. Time shown is relative to the ablation pulse. The overall exponential decay in absorption is due to diffusion to the cell walls, where the titanium atoms adsorb. The sudden decrease in optical density at 0.25 s is due to the optical pumping beam, which was on from 249 ms to 250 ms. The increase in optical density following optical pumping is due to Ti-He collisions returning atoms from the $a\ ^3F_3$ state to the $a\ ^3F_2$.

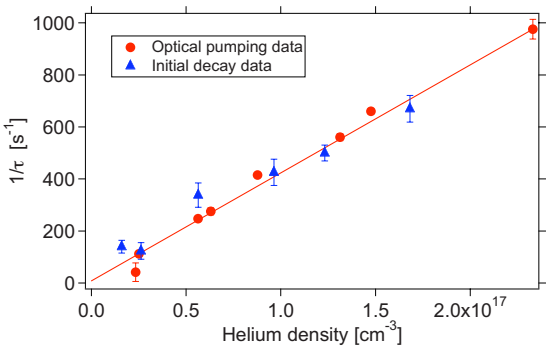

FIG. 4. (Color online) $1/\tau_{3\rightarrow 2}$ as a function of helium gas density, at a cell temperature of 5 K. The line is a least-squares fit to $1/\tau = k n_{\mathrm{He}}$. Error bars are a combination of statistical error and an estimate of systematic error due to diffusion of atoms in and out of the volume of the pumping beam. There is an overall uncertainty in the helium density of ±15%.

The return to equilibrium is fit to

$$\dot{N}_3 = -\frac{N_3}{\tau_D} - \frac{N_3}{\tau_{3\rightarrow 2}}; \quad \dot{N}_2 = -\frac{N_2}{\tau_D} + \frac{N_3}{\tau_{3\rightarrow 2}},$$

where τ_D is the diffusion time constant. The inelastic collision time scales τ are related to the collision rate coefficient by $k_{3\rightarrow 2} = (n_{\mathrm{He}}\tau_{3\rightarrow 2})^{-1}$, where n_{He} is the helium density. The $J=4$ population is ignored because it is negligibly small under these conditions. The neglected "inverse" process $\tau_{2\rightarrow 3}$ can be calculated from the $\tau_{3\rightarrow 2}$ rate and the principle of detailed balance [20]. At the temperatures of our experiments it is sufficiently small that it may be neglected, and is omitted from our fit.

As seen in Fig. 4, $1/\tau_{3\rightarrow 2}$ scales linearly with the helium density, so we conclude the return to $J=2$ is due to collisions with helium. To confirm this measurement, we measured $\tau_{3\rightarrow 2}$ under different experimental conditions. We found $\tau_{3\rightarrow 2}$ is independent of the ablation energy (measured over the range 5 mJ to 50 mJ) and independent of the time delay with respect to the ablation pulse (measured over 0.1 s to 1.5 s), indicating that the collisions are not with substances produced by the ablation pulse. Similarly, $\tau_{3\rightarrow 2}$ is independent of pumping beam direction and diameter, as long as the pumping beam is sufficiently large that diffusion in and out of the pumping beam volume plays a small role on the time scale of the collisional return to equilibrium. $\tau_{3\rightarrow 2}$ is also independent of the pumping duration, as long as the pumping time is not significantly longer than the collisional relaxation time, as explained below.

Unfortunately, there are a large number of metastable states between the $a\ ^3F$ ground state and $y\ ^3F_2$ excited state. Fortunately, decay back to the $a\ ^3F$ ground state is the dominant decay path [18]. By using a pumping duration which is short compared to the collisional relaxation time, we ensure the majority of atoms which are removed from $a\ ^3F_2$ are pumped into the $a\ ^3F_3$ state. If we pump for times much longer than the time scale for collisional relaxation of the $a\ ^3F_3$ level, we begin to accumulate significant numbers of

TABLE I. Ti-He $J=3\rightarrow J=2$ inelastic collision rate coefficient k at different temperatures T. Experimental error is a combination of statistical error and estimates of systematic error, which is primarily due to uncertainty in the helium density.

	Theory	Experiment
T (K)	$k_{3\rightarrow 2}$ (cm^3 s^{-1})	$k_{3\rightarrow 2}$ (cm^3 s^{-1})
5.2	1.86×10^{-15}	$(4.4\pm 0.7)\times 10^{-15}$
9.9	2.74×10^{-15}	$(5.3\pm 0.8)\times 10^{-15}$
15.6	4.50×10^{-15}	$(7.7\pm 1.2)\times 10^{-15}$
19.9	6.18×10^{-15}	$(9.8\pm 1.5)\times 10^{-15}$

atoms in other, unknown, metastable states. Decay from these higher-energy states can be distinguished from our levels of interest because it is accompanied by visible fluorescence from the cell; the decay from $a\ ^3F_3$ exhibits no such visible light. To avoid complications from such effects, we only use data taken with short pumping durations.

As a secondary measurement technique, we directly monitor the $J=3$ population with absorption spectroscopy. Large numbers of $J=3$ atoms are produced in the initial ablation pulse, but relax to the $J=2$ level due to inelastic fine-structure relaxation collisions. By comparing the lifetimes of $J=3$ atoms and $J=2$ atoms, and fitting to our above model, we can extract values of $\tau_{3\rightarrow 2}$. Data obtained through this "initial decay" method is shown alongside optical pumping data in Fig. 4; the two are consistent within our experimental error.

To determine collision cross sections and rate coefficients from τ, we need to measure the density of helium in the cell. We measure the pressure in a Pirani gauge at 300 K which is connected to the cell by a thin fill line. The gauge pressure is higher than the actual cell pressure due to the thermomolecular pressure ratio; we determine the cell pressure by the Weber-Schmidt equation [21,22]. We determine the density from this adjusted pressure, the cell temperature, and the ideal gas law. An independent determination of the cell buffer-gas density from the known quantity of helium introduced into the cell yields densities that agree with the Weber-Schmidt value to within $\sim$10%.

The measured rate coefficients for inelastic Ti-He collisions at different temperatures are shown in Table I, along with theoretically predicted values.

TABLE II. Thermally averaged Ti-He cross sections $\bar{\sigma}$. The first and second columns are theoretical estimates for the total elastic and diffusion cross sections, respectively. The third column lists experimental values for the diffusion cross section; the dominant source of error is due to approximations made in the modeling of diffusion in the cell geometry [24].

	Theory		Experiment
T (K)	$\bar{\sigma}_e$ (cm^2)	$\bar{\sigma}_d$ (cm^2)	$\bar{\sigma}_d$ (cm^2)
5.2	5.10×10^{-14}	1.50×10^{-14}	$(1.1\pm 0.3)\times 10^{-14}$
9.9	3.72×10^{-14}	1.05×10^{-14}	$(8.6\pm 2.3)\times 10^{-15}$
15.6	2.99×10^{-14}	8.68×10^{-15}	$(7.7\pm 2.1)\times 10^{-15}$
19.9	2.67×10^{-14}	7.95×10^{-15}	$(7.3\pm 2.0)\times 10^{-15}$

In our theoretical calculations of Ti-He collisions, the interaction between the Ti-He collision partners is given by the multichannel potential matrix [23]

$$\underline{V}(R,\theta,\phi)=\sum_{\Omega_1}[j,j']^{1/2}\mathcal{D}^{j}_{\Omega\Omega_1}(\theta,\phi)\mathcal{D}^{j'}_{\Omega_1\Omega'}(-\theta,\phi)\times\sum_{\Lambda M_S}\begin{pmatrix}L & S & j\\ \Lambda & M_S & -\Omega_1\end{pmatrix}\begin{pmatrix}L & S & j'\\ \Lambda & M_S & -\Omega_1\end{pmatrix}\epsilon_\Lambda(R), \tag{1}$$

where $\mathcal{D}^{j}_{\Omega\Omega'}(\theta,\phi)$ is a Wigner rotation matrix [23], j,Ω are total, and azimuthal, electronic angular momentum quantum numbers for the TiHe diatom, $\epsilon_\Lambda(R)$ are the Born-Oppenheimer potentials corresponding to its Σ, Π, Δ, and Φ ground electronic states [13], $L=3$, $S=1$, and $[j]$ is shorthand for $2j+1$. The Born-Oppenheimer potentials are adiabatic, and in this calculation we have neglected nonadiabatic couplings due to nuclear motion, which are expected to be small.

We can reexpress the excited state potentials in terms of their energy defect $\delta_i(R)$ with the ground energy, i.e., $\epsilon_i(R)=\epsilon_\Sigma(R)+\delta_i(R)$. In this parametrization Eq. (1) becomes

$$\underline{V}(R,\theta,\phi)=\delta_{j,j'}\delta_{\Omega,\Omega'}\epsilon_\Sigma(R)+\underline{W}(R,\theta,\phi), \tag{2}$$

where the first term is a consequence of the unitary property of the Wigner matrices and orthogonality of the $3j$ symbols [23]. $\underline{W}(R,\theta,\phi)$ has the same form as Eq. (1), except that $\epsilon_i(R)$ is replaced by $\delta_i(R)$. This anisotropic component depends on the orientation (θ,ϕ) of the collision axis, as well as the internuclear separation R. It is proportional to the effective "coupling" terms δ_i, and induces fine-structure-changing transitions [23]. *Ab initio* calculations by Kłos *et al.* [13] have shown that the energy splittings δ_i are extremely small, on the order of 0.1 cm^{-1}, due to the fact that the $3d$ valence electrons in Ti "submerge" under the doubly filled $4s$ subshell. In contrast, splittings on the order of tens of cm^{-1}, such as seen in the O(^3P)-He system are typical [12]. The latter lead to enhanced angular momentum transfer during a collision. In Tables I and II, we find reasonable agreement with our experimental data and the theoretical predictions obtained using the *ab initio* potentials of Kłos *et al.* [13]. The magnitudes of the predicted cross sections and their collision energy dependence is consistent with experiment. The theoretical calculations underestimate the measured cross sections by a factor of 2.4 at lower energies, and predicts 63% of the measured value at 19.9 K. If we introduce a small rescaling of the *ab initio* potentials, we can obtain better agreement with the experimental data [23].

From our data, we can also extract Ti-He elastic collision cross sections. At low helium pressures, and at times long after the ablation pulse, the number of atoms in the cell is observed to decay exponentially in time, and the exponential lifetime scales linearly with the density of helium. This is the expected behavior for atom loss due to diffusion to the cell walls, where they are expected to stick [24]. At higher pressures ($n\gtrsim 3\times 10^{17}$ cm^{-3}), the behavior of the titanium atoms begins to deviate from the expected diffusion behavior, similar to what was recently reported by Sushkov and Budker

[25]. We determine diffusion cross sections from diffusion lifetimes measured at helium densities ranging from 7×10^{15} cm^{-3} to 2×10^{17} cm^{-3}. Values are shown in Table II, alongside theoretically calculated values.

In conclusion, we have measured the Ti-He fine-structure-changing inelastic collision rate coefficient at cryogenic temperatures. The collision rate coefficient is roughly three orders of magnitude smaller than previous measurements of cold fine-structure relaxation collisions in nonsubmerged shell atoms C, Si, and Al [5,4].

The Ti-He collisional J relaxation is significantly slower than m relaxation. Reference [12] measured the Ti-He Zeeman-relaxation rate coefficient at 1.8 K and 3.8 T, and found $k_m = (1.1 \pm 0.7) \times 10^{-14}$ cm^3 s^{-1}. Our repetition of those measurements at 5 K and fields of a few gauss indicate a rate coefficient of $k_m = (1.2 \pm 0.6) \times 10^{-13}$ cm^3 s^{-1}. At present, it is unknown if this large disparity in the relative strength of m-changing and J-changing collisions is general for all atoms with fine structure, or if it is specific to the Ti-He system.

The experimental technique employed in this work—a combination of laser ablation, buffer gas cooling, and optical pumping—should be applicable to measuring fine-structure-changing collisions between atoms and helium for any spectroscopically addressable species. We have shown its efficacy in an atom without a closed optical transition. This technique should be of use for measuring a wide variety of cold collision processes in a wide range of atoms and molecules. Extrapolating from our current measurements, we expect to be able to measure inelastic collisions ranging from 10^{-10} to 10^{-17} cm^3 s^{-1}, at temperatures down to roughly 0.5 K [15].

We gratefully acknowledge helpful discussions with John M. Doyle and Roman V. Krems. We thank Jacek Kłos for providing the Ti-He molecular potentials. We thank William A. Brinsmead, Wade J. Cline, and Dennis J. Meredith for technical assistance. This work was financially supported by the University of Nevada, Reno. B.Z. was supported, in part, by the Department of Energy under Contract No. DE-FG36-05GO85028.

[1] A. Dalgarno and R. McCray, Annu. Rev. Astron. Astrophys. **10**, 375 (1972).
[2] D. Flower, *Molecular Collisions in the Interstellar Medium* (Cambridge University Press, Cambridge, 2003).
[3] E. Abrahamsson *et al.*, Astrophys. J. **654**, 1171 (2007).
[4] S. D. L. Picard *et al.*, J. Chem. Phys. **108**, 10319 (1998).
[5] S. D. L. Picard *et al.*, J. Chem. Phys. **117**, 10109 (2002).
[6] C. I. Hancox *et al.*, Nature (London) **431**, 281 (2004).
[7] D. Hansen and A. Hemmerich, Phys. Rev. Lett. **96**, 073003 (2006).
[8] R. Chicireanu *et al.*, Phys. Rev. A **76**, 023406 (2007).
[9] A. Derevianko *et al.*, Phys. Rev. Lett. **90**, 063002 (2003).
[10] V. Kokoouline, R. Santra, and C. H. Greene, Phys. Rev. Lett. **90**, 253201 (2003).
[11] R. V. Krems, J. Klos, M. F. Rode, M. M. Szczesniak, G. Chalasinski, and A. Dalgarno, Phys. Rev. Lett. **94**, 013202 (2005).
[12] C. I. Hancox, S. C. Doret, M. T. Hummon, R. V. Krems, and J. M. Doyle, Phys. Rev. Lett. **94**, 013201 (2005).
[13] J. Klos *et al.*, Eur. Phys. J. D **31**, 429 (2004).
[14] J. Kim, B. Friedrich, D. P. Katz, D. Patterson, J. D. Weinstein, R. deCarvalho, and J. M. Doyle, Phys. Rev. Lett. **78**, 3665 (1997).
[15] R. deCarvalho *et al.*, Eur. Phys. J. D **7**, 289 (1999).
[16] J. K. Messer and F. C. D. Lucia, Phys. Rev. Lett. **53**, 2555 (1984).
[17] A. Hatakeyama, K. Enomoto, and T. Yabuzaki, Phys. Scr., T **110**, 294 (2004).
[18] Y. Ralchenko *et al.*, *NIST Atomic Spectra Database*, 3rd ed. (National Institute of Standards and Technology, Gaithersburg, MD, 2007).
[19] Lake Shore Cryotronics DT-670-CU-1.4D.
[20] D. Chandler, *Introduction to Modern Statistical Mechanics* (Oxford University Press, Oxford, 1987).
[21] S. Weber and G. Schmidt, Leiden Comm., No. **246c** (1936).
[22] T. R. Roberts and S. G. Sydoriak, Phys. Rev. **102**, 304 (1956).
[23] B. Zygelman, Phys. Rev. A (to be published).
[24] J. B. Hasted, *Physics of Atomic Collisions*, 2nd ed. (American Elsevier, New York, 1972).
[25] A. O. Sushkov and D. Budker, Phys. Rev. A **77**, 042707 (2008).